

Towards hexagonal C_{2v} systems with anisotropic DMI: Characterization of epitaxial Co(10.0)/Pt(110) multilayer films

Yukun Liu, Michael D. Kitcher, Marc De Graef, and Vincent Sokalski
*Department of Materials Science & Engineering,
 Carnegie Mellon University, Pittsburgh, PA, USA 15213*
 (Dated: March 1, 2022)

Ferromagnet/heavy metal multilayer thin films with C_{2v} symmetry have the potential to host antiskyrmions and other chiral spin textures via an anisotropic Dzyaloshinskii-Moriya interaction (DMI). Here, we present a candidate material system that also has a strong uniaxial magnetocrystalline anisotropy aligned in the plane of the film. This system is based on a new Co/Pt epitaxial relationship, which is the central focus of this work: hexagonal closed-packed Co(10.0)[00.1] || face-centered cubic Pt(110)[00.1]. We characterized the crystal structure and magnetic properties of our films using X-ray diffraction techniques and magnetometry respectively, including q-scans to determine stacking fault densities and their correlation with the measured magnetocrystalline anisotropy constant and thickness of Co. In future ultrathin multilayer films, we expect this epitaxial relationship to further enable an anisotropic DMI and interfacial perpendicular magnetic anisotropy. The anticipated confluence of these properties, along with the tunability of multilayer films, make this material system a promising testbed for unveiling new spin configurations in FM/HM films.

I. INTRODUCTION

Magnetic skyrmions are promising candidates for future spintronic data storage and logic devices because of their small size, heightened stability, and high mobility [1–5]. These structures are typically stabilized via the Dzyaloshinskii-Moriya Interaction (DMI) which emerges in magnetic systems with high spin-orbit coupling and no inversion symmetry [6–8]. In polycrystalline ferromagnet/heavy metal (FM/HM) thin films, only Néel skyrmions have been stabilized due to the high symmetry of these systems [2, 3, 5, 7, 9–14]. However, recent research suggests that antiskyrmions—the topological opposites of skyrmions—can be stabilized by anisotropic DMI that arises at FM/HM thin film interfaces with low symmetry [12–16]. Specifically, antiskyrmions are preferred over Néel skyrmions when the DMI has opposing signs along orthogonal crystallographic directions. To date, research on anisotropic DMI in FM/HM systems has focused on films based on a body-centered cubic (BCC) heavy metal [13, 15–19]. Moreover, across the limited experimental studies carried out thus far, a suitable antiskyrmion host has not been found.

To expand this search, we present a system that exhibits the growth of hexagonal close-packed (HCP) cobalt on a face-centered cubic (FCC) Pt underlayer, with a singular magnetocrystalline easy axis lying in the plane of the film. The presence of this in-plane uniaxial anisotropy is likely to broaden the range of possible spin configurations that could exist when coupled with a significant, potentially anisotropic DMI and/or an interface-induced perpendicular easy axis. In this work, we characterized the epitaxial relationship that enables such a system; investigated the prevalence of structural defects—namely, intrinsic stacking faults (SFs)—during the growth of films; and measured the magnetocrystalline anisotropy (MCA) by probing the resulting in-plane hysteresis behavior.

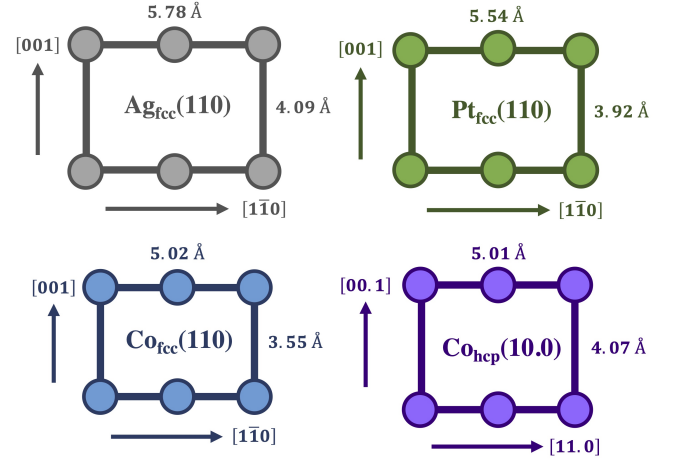


FIG. 1. Orientation and interatomic relationship between FCC Ag(110), FCC Pt(110), FCC Co(110), and HCP Co(10.0).

II. METHODS

All films were grown via DC magnetron sputtering in an Ar atmosphere at a fixed working pressure of 2.5 mTorr. Prior to deposition, Si(110) single-crystal substrates were HF-etched for 1 minute to remove any native oxide that would otherwise degrade the epitaxial growth. Following Yang et al., we deposit a Ag buffer layer which is expected to grow with the (110) texture on Si(110) [20]. This growth seed facilitates the deposition of our films at room temperature, thus avoiding the severe inter-layer diffusion that occurs at elevated temperatures [20]. Moreover, the degree of lattice mismatch between Ag and Pt is rather moderate ($\sim 4.3\%$). Pt[10 nm]/Co[20 nm],

50 nm]/Pt[3 nm] thin films were subsequently deposited. To identify the phases and textures of the different layers, 2θ - ω coupled scans and azimuthal (φ) scans were performed on the deposited thin films using a Phillips X'Pert Pro diffractometer. Furthermore, the density of SFs in HCP Co for each sample was quantitatively determined from X-ray reciprocal space q -scans. Using measurements of the full width at half maximum (w_h) of different Co peak profiles along different directions, we extracted the broadening effects caused by different intrinsic SFs. The corresponding SF densities were subsequently calculated.

The magnetic anisotropy of the deposited thin films was examined using a Princeton Measurements alternating gradient force magnetometer (AGFM). M - H hysteresis curves were obtained for orthogonal in-plane directions and their corresponding magnetic anisotropy energy densities were calculated from the area between one half of the idealized hard axis and the M -axis.

III. RESULTS AND DISCUSSION

The representative 2θ - ω coupled scan profiles presented in Figure 2 show dominant HCP Co($10\bar{1}0$), FCC Pt(220), and FCC Ag(220) diffraction peaks, indicating that while Pt grows with the same preferred FCC (110) orientation of the Ag underlayer, Co adopts the HCP ($10\bar{1}0$) texture. These results are corroborated by the azimuthal scan profiles in Figure 3 which reveal HCP Co($10\bar{1}1$) planes at the same azimuth as FCC (111) planes in Pt and Ag. Correspondingly, the epitaxial relationship between layers is Co($10\bar{1}0$)[0001] \parallel Pt(110)[001] \parallel Ag(110)[001] \parallel Si(110)[001]. The strong (110) texture of the Ag growth seed in these films agrees with the work of Yang et al., who noted that a 4×4 mesh of Ag unit cells on a 3×3 mesh of Si unit cells has a lattice mismatch of less than 0.45% [20].

Given the prevalence of “all-FCC” Co/Pt multilayers used in magnetics research, it may seem counterintuitive that a Pt(110) underlayer would give rise to a hexagonal Co layer. However, as shown in Figure 1, the Co($10\bar{1}0$) surface has a significantly higher degree of lattice matching along [001] with the Pt(110) surface as compared to its FCC (110) counterpart, while the mismatches along [110] are nearly identical. Together with cobalt’s thermodynamic preference for the HCP phase at the deposition temperature, the potential for a lower strain drives the formation of the observed texture. However, the theoretical lattice mismatch along $[1\bar{1}0]$ at the predicted Co/Pt interface is considerable. We therefore explored the prevalence of intrinsic SFs in these films and their impact on the magnetocrystalline uniaxial anisotropy along the c -axis of Co.

It has been established that intrinsic SFs in HCP crystals broaden diffraction peaks along [0001] when $H - K \neq 3N$, where $N \in \mathbb{Z}$. Furthermore, the degree of broadening depends on the parity of L . Specifically, the

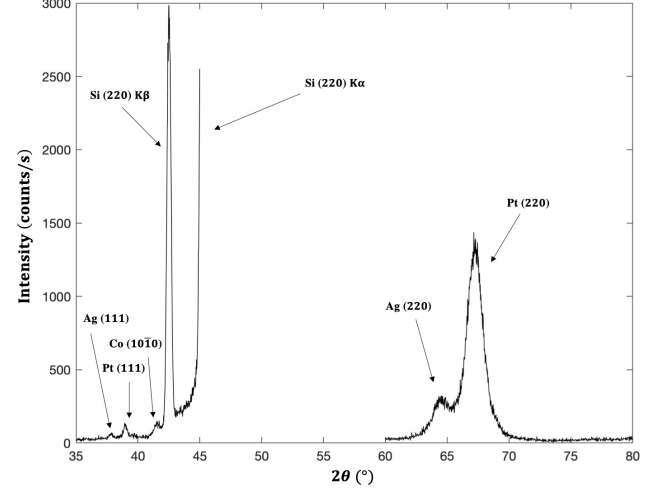


FIG. 2. Diffraction profiles of 2θ - ω coupled scans performed on the Co(20 nm)/Pt film

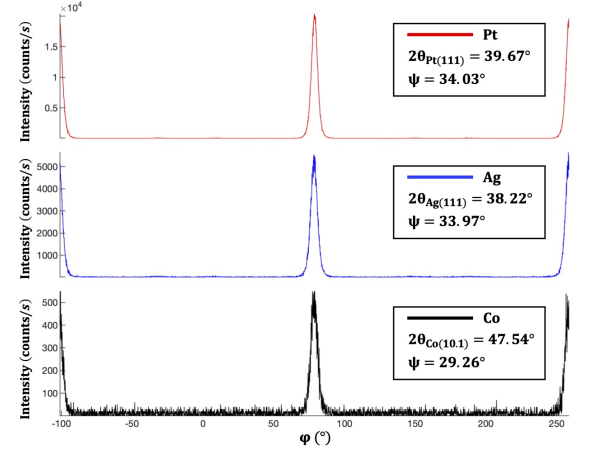


FIG. 3. Diffraction profiles of azimuthal (φ) scans performed on the Co(20 nm)/Pt film.

normalized broadening, $\Delta w_{h,sf}$, of these peaks in reciprocal space and the density of SFs are related by

$$\Delta w_{h,sf} = \frac{3\alpha + 3\beta}{\pi}, \quad L \bmod 2 = 0 \quad (1)$$

$$\Delta w_{h,sf} = \frac{3\alpha + \beta}{\pi}, \quad L \bmod 2 = 1 \quad (2)$$

where α and β represent the densities of deformation and growth SFs, respectively [21]. However, the diffraction profile of a reciprocal space q -scan is also affected by the broadening effect caused by mosaicity; the observed broadening must therefore be deconvolved during this analysis. A summary of the possible broadening effects for different peaks is shown in Table I.

we note that lattice strain along the $\text{Co}[11\bar{2}0]$ direction may also influence the values of K_u magnetoelastically. These results support the possibility of a significant uniaxial in-plane MCA in thinner films. Since chiral spin structures have been observed in ultrathin FCC (111) Co/Pt films due to interfacial DMI (which is nominally anisotropic in C_{2v} films) and perpendicular magnetic anisotropy (PMA), one could capitalizing on the tunability of multilayer systems and potentially explore the interplay between all three effects in ultrathin films based on this HCP-FCC Co/Pt system.

TABLE II. The combined deformation (α) & growth (β) stacking fault densities and the magnetocrystalline anisotropy energy density, K_u , for each deposited film.

Film	$\alpha + \beta$ (%)	K_u (kJ/m ³)
Co[20 nm]/Pt	7.644	64.8
Co[50 nm]/Pt	9.142	52.4

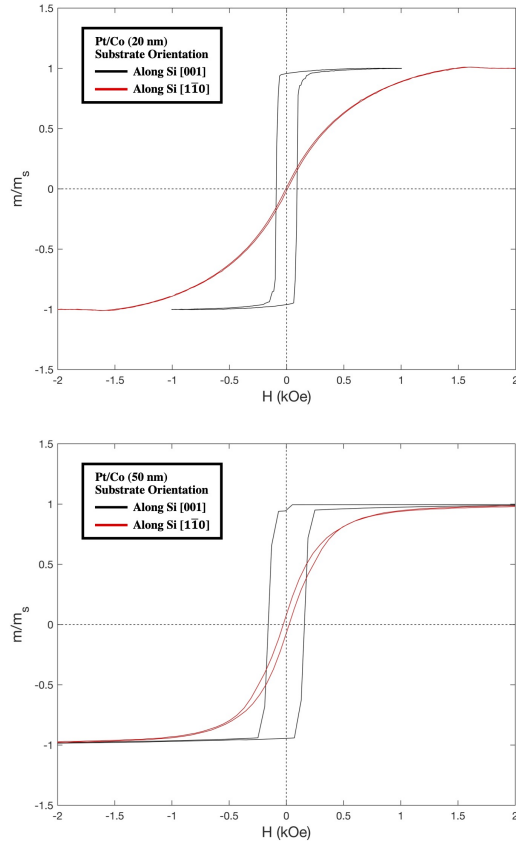


FIG. 6. Measured M-H hysteresis curves for Co/Pt films. The thickness of the cobalt layer in each film is given in parentheses. The measurement directions are indicated with respect to the Si substrate.

IV. CONCLUSION

In this work, we characterized Co(20nm)/Pt and Co(50nm)/Pt C_{2v} films sputtered at room temperature on Si(110) substrates with a Ag growth seed. The epitaxial relationship between the Pt and Co layers was identified as HCP $\text{Co}(10\bar{1}0)[0001] \parallel \text{FCC Pt}(110)[001]$; to our knowledge, this is the first report of an HCP \parallel FCC FM/HM epitaxial film system. These films exhibit a definitive uniaxial in-plane magnetic anisotropy along the $\text{Si}[110]$ direction, in agreement with the observed HCP $(10\bar{1}0)$ texture of Co. An analysis of the broadening of $\text{Co}(10\bar{1}0)$ peaks along principal directions revealed stacking fault densities of 7.6% and 9.1% in the 20 nm and 50 nm films, respectively. Both films have significantly lower K_u values compared to bulk cobalt, which we attribute, at least in part, to the appreciable intrinsic stacking fault densities observed. We anticipate that the observed epitaxial relationship and the singular in-plane easy axis will be preserved in thinner films, where the collective impact of interface-induced PMA, anisotropic DMI and in-plane uniaxial anisotropy on chiral spin structures in multilayer thin films could be explored.

V. ACKNOWLEDGEMENTS

All authors acknowledge the support of the Defense Advanced Research Agency (DARPA) program on Topological Excitations in Electronics (TEE) (Grant No. D18AP00011), as well as the use of the Materials Characterization Facility at Carnegie Mellon University supported by grant MCF-677785. M.D.K. is also grateful for the support of the National GEM Consortium, as well as the support of the Neil and Jo Bushnell Engineering Fellowship awarded by Carnegie Mellon University's College of Engineering.

-
- [1] A. Fert, V. Cros, and J. Sampaio, *Nature Nanotechnology* **8**, 152–156 (2013).
 - [2] N. Nagaosa and Y. Tokura, *Nature Nanotechnology* volume **8**, 899–911 (2013).
 - [3] K. Everschor-Sitte, J. Masell, R. M. Reeve, and M. Kläui, *Journal of Applied Physics* **124**, 240901 (2018).
 - [4] D. Prychynenko, M. Sitte, K. Litzi, B. Krüger, G. Bourianoff, M. Kläui, J. Sinova, and K. Everschor-Sitte, *Physical Review Applied* **9**, 014034 (2018).
 - [5] C. Back, V. Cros, H. Ebert, K. Everschor-Sitte, A. Fert, M. Garst, T. Ma, S. Mankovsky, T. L. Monchesky, M. Mostovoy, N. Nagaosa, S. S. P. Parkin, C. Pfleiderer, N. Reyren, A. Rosch, Y. Taguchi, Y. Tokura, K. von Bergmann, and J. Zang, *Nature Physics* **7**, 713–718 (2011).
 - [6] I. E. Dzyaloshinskii, *Journal of Physics and Chemistry of Solids* **4**, 241–255 (1958).
 - [7] T. Moriya, *Physical Review* **120**, 91–98 (1960).
 - [8] U. K. Rößler, A. N. Bogdanov, and C. Pfleiderer, *Nature* **442**, 797–801 (2006).
 - [9] S. Mühlbauer, B. Binz, F. Jonietz, C. Pfleiderer, A. Rosch, A. Neubauer, R. Georgii, and P. Böni, *Science* **323**, 915–919 (2009).
 - [10] X. Yu, Y. Onose, N. Kanazawa, J.-H. Park, J. H. Han, Y. Matsui, N. Nagaosa, and Y. Tokura, *Nature* **465**, 901–904 (2010).
 - [11] S. Heinze, K. V. Bergmann, M. Menzel, J. Brede, A. Kubetzka, R. Wiesendanger, G. Bihlmayer, and S. Blügel, *Nature Physics* **7**, 713–718 (2011).
 - [12] U. Güngördü, R. Nepal, O. A. Tretiakov, K. Belashchenko, and A. A. Kovalev, *Physical Review B* **93**, 064428 (2016).
 - [13] M. Hoffmann, B. Zimmermann, and G. P. Müller, *Nature Communications* **8**, 308 (2017).
 - [14] A. Raeliarijaona, R. Nepal, and A. A. Kovalev, *Physical Review Materials* **2**, 124401 (2018).
 - [15] L. Camosi, S. Rohart, O. Fruchart, S. Pizzini, M. Belmeguenai, Y. Roussigné, A. Stashkevich, S. M. Cherif, L. Ranno, M. de Santis, and J. Vogel, *Physical Review B* **95**, 214422 (2017).
 - [16] S. Huang, C. Zhou, G. Chen, H. Shen, A. K. Schmid, K. Liu, and Y. Wu, *Physical Review B* **96**, 144412 (2017).
 - [17] L. Camosi, N. Rougemaille, O. Fruchart, J. Vogel, and S. Rohart, *Physical Review B* **97**, 134404 (2018).
 - [18] L. Camosi, J. Peña-Garcia, O. Fruchart, S. Pizzini, A. Locatelli, T. O. Mentes, F. Genuzio, H. N. Justin Shaw, and J. Vogel, *New Journal of Physics* **23**, 013020 (2021).
 - [19] S. Tsurkan and K. Zakeri, *Physical Review B* **102**, 060406(R) (2020).
 - [20] W. Yang, D. N. Lambeth, and D. E. Laughlin, *Journal of Applied Physics* **85**, 8 (1999).
 - [21] M. T. Sebastian and P. Krishna, *Random, Non-Random and Periodic Faulting in Crystals* (Gordon and Breach Science Publishers, 1994).
 - [22] B. D. Cullity and J. Chad D. Graham, *Introduction to Magnetic Materials* (Wiley-IEEE Press, 2008) p. 227.